Chemical Data Collections 27 (2020) 100384

Contents lists available at ScienceDirect

Chemical Data Collections

journal homepage: www.elsevier.com/locate/cdc

Data on Chloride-related electrochemical deterioration of micro-alloyed steel in E20 simulated fuel ethanol blend

Olufunmilayo O. Joseph[a,*], John Ade Ajayi[b]

[a] Department of Mechanical Engineering, Covenant University, P.M.B. 1023, Canaanland, Ota, Nigeria
[b] Department of Metallurgical and Materials Engineering, Federal University of Technology, Akure, P.M.B. 704, Akure, Nigeria

ARTICLE INFO

Article history:
Received 27 January 2020
Revised 29 March 2020
Accepted 30 March 2020
Available online 21 April 2020

Keywords:
Chloride
Fuel ethanol
Corrosion rate
Polarization

ABSTRACT

The data existing in this work relate to the study (Chloride effects on the electrochemical degradation of micro-alloyed steel (MAS) in E20 simulated fuel ethanol blend (SFGE) (Joseph, 2017) [1]. Corrosion rates of MAS versus chloride concentration in E20 are presented. Potentiodynamic polarization tests data were also covered. Composition analysis of the corrosion products as well as images of the samples' surfaces before and after testing were also presented. The calculations are based on ASTM Standard G1-03 for determining mass loss and corrosion rates. Data are valuable to assess that there is increase in corrosion rate with increase in chloride. Hence, it is noted that chloride could be reduced to the barest minimum in fuel ethanol. Pitting form of corrosion are presented in the scanning electron microscopic images.

Specifications Table

Subject area	*Materials Science and Engineering*
Compounds	*195 proof ethanol, gasoline, sodium chloride, methanol, acetic acid*
Data category	*Physicochemical*
Data acquisition format	*FEI-430 NOVA NANO FEG-SEM, Gamry Reference 600 Potentiostat/Galvanostat, Bruker D8 Discover X-ray Diffractometer*
Data type	*Raw, analysed*
Procedure	*Anodic polarization tests via potentiostatic analysis, weight loss measurements, corrosion rate determination, surface characterisation*
Data accessibility	*Data are available within this article*

1. Rationale

In order to solve the problem of global warming in the world today, biofuels are currently being used as an alternative to fossil fuels. Generally, biofuels such as ethanol offers great advantages due to their chemical as well as physical characteristics, low production costs, raw materials availability and environmental friendly effects, amongst several others [2-4]. Conversely, ethanol has certain drawbacks as regards material compatibility. When ethanol is present in fuel, the fuel's chemical composition may cause corrosion on some parts of the automotive engine. As a result, materials which normally would not corrode in gasoline may be damaged by the presence of ethanol. In spite of the substantial number of tests

* Corresponding author.
E-mail address: funmi.joseph@covenantuniversity.edu.ng (O.O. Joseph).

https://doi.org/10.1016/j.cdc.2020.100384

Table 1
OCP Data for micro-alloyed steel in E20 + 0 mg/L NaCl.

Pt #	T s	Vf (final voltage) V vs. Ref. (E-02)	Vm (measured voltage) V (E + 00)	Ach Offset V (E-04)
0	0.26	−4.89	0.00	4.19
1	0.52	−4.89	0.00	4.16
2	0.78	−4.89	0.00	4.14
3	1.03	−4.89	0.00	4.16
4	1.29	−4.89	0.00	4.14
5	1.55	−4.89	0.00	4.15
6	1.81	−4.89	0.00	4.13
7	2.07	−4.89	0.00	4.18
8	2.33	−4.89	0.00	4.18
9	2.58	−4.89	0.00	4.18
10	2.84	−4.89	0.00	4.17
11	3.10	−4.89	0.00	4.21
12	3.36	−4.89	0.00	4.19
13	3.62	−4.89	0.00	4.18
14	3.88	−4.89	0.00	4.16
15	4.13	−4.89	0.00	4.17
16	4.39	−4.89	0.00	4.14
17	4.65	−4.89	0.00	4.16
18	4.91	−4.89	0.00	4.17
19	5.17	−4.89	0.00	4.09
20	5.43	−4.89	0.00	4.15
21	5.68	−4.89	0.00	4.17
22	5.94	−4.89	0.00	4.13
23	6.20	−4.89	0.00	4.18
24	6.46	−4.89	0.00	4.18
25	6.72	−4.89	0.00	4.17
26	6.98	−4.89	0.00	4.16
27	7.23	−4.89	0.00	4.16
28	7.49	−4.89	0.00	4.15
29	7.75	−4.89	0.00	4.18
30	8.01	−4.89	0.00	4.16
31	8.27	−4.89	0.00	4.18
32	8.53	−4.89	0.00	4.15
33	8.78	−4.89	0.00	4.14
34	9.04	−4.89	0.00	4.16
35	9.30	−4.89	0.00	4.18
36	9.56	−4.89	0.00	4.17
37	9.82	−4.89	0.00	4.22
38	10.08	−4.89	0.00	4.19

[5-12] conducted so far to study corrosion mechanisms in fuel ethanol, there are still growing concerns about the corrosion behaviour of pipeline materials used to handle fuel ethanol. Due to increased complication and multiplicity of material classifications (such as composites, ceramics, polymers and metallic materials), the effect of corrosion on civilization and the accompanying material degradation are far reaching [13]. This research work addresses the importance of failure analysis and prevention with focus on identifying critical failure modes in fuel ethanol environments and establishing corrosion rates of MAS in the environment of consideration.

The data are valuable for the assessment of the deteriorating effect of chloride in E20 SFGE on micro-alloyed steel material. The data regarding mass loss corrosion rate and instantaneous corrosion rate are useful to Engineers in designing against failure. This data regarding the simulated fuel ethanol blend can be compared with data on plant fuel ethanol blend for further insight. The data in this article which is based on three chloride concentrations can be used to develop further experiments in considering much wider chloride concentrations.

2. Procedure

Experimental details are presented in Joseph, 2017 [1]. The method used is as described in [14-16] for formulating, cleaning and evaluation of corrosion test coupons. The E20 SFGE was primed according to ASTM Standard D-4806–07 for fuel grade ethanol which consist of: methanol (0.5 vol.%); acetic acid (56 mg/L); NaCl (32 mg/L); water (1 vol.%) and ethanol (98.5 vol.%) [1,17]. The denaturant used was unleaded gasoline. Chloride concentration was adjusted to simulate the various test conditions. Even square specimens of (30 × 30 × 11) mm dimensions were used for the mass loss tests. For this data, initial and final weight measurements of samples were taken during immersion tests (a total of six samples) and average value was computed for mass loss from respective duos of replica test. Afterwards, corrosion rate was calculated in mpy

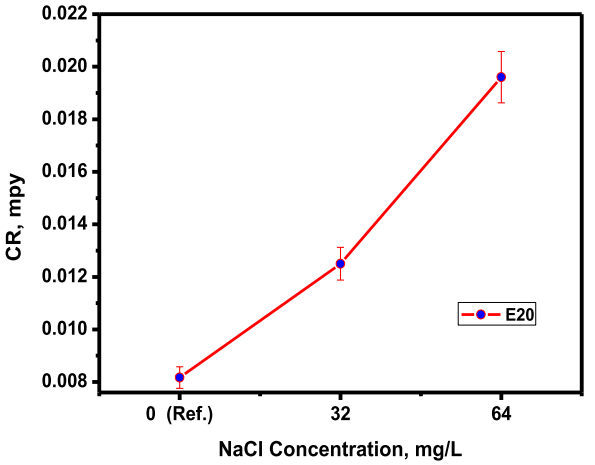

Fig. 1. Relationship between corrosion rate and chloride concentration for MAS in E20. Error bars show standard deviation.

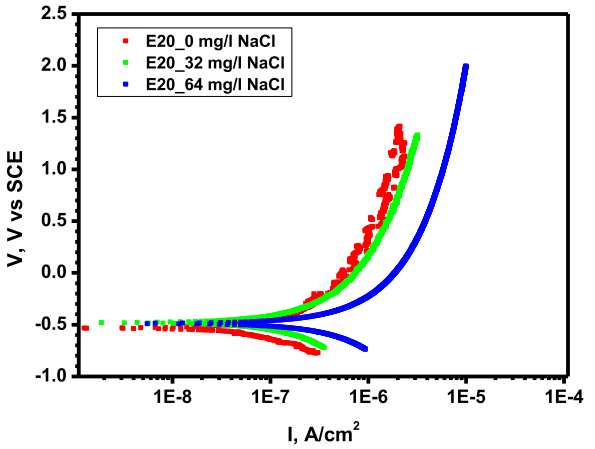

Fig. 2. Anodic polarization data for MAS in E20 with and without chloride.

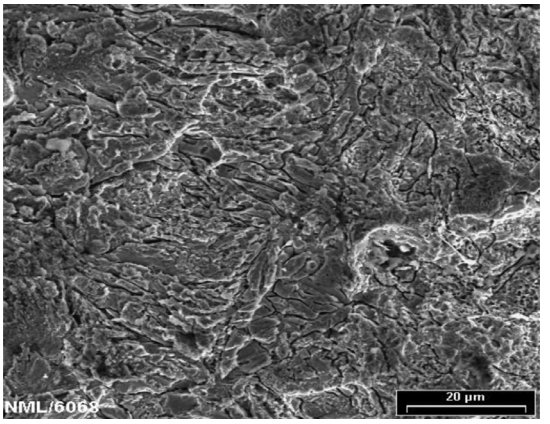

Fig. 3. No pits on MAS following immersion test in the absence of chloride.

Table 2
OCP Data for micro-alloyed steel in E20 + 32 mg/L NaCl.

Pt #	T s	Vf V vs. Ref. (E-01)	Vm V (*E* + 00)	Ach V (E-04)
0	0.26	−5.26	0.00	−2.47
1	0.52	−5.26	0.00	−2.49
2	0.78	−5.26	0.00	−2.50
3	1.03	−5.26	0.00	−2.49
4	1.29	−5.26	0.00	−2.48
5	1.55	−5.26	0.00	−2.47
6	1.81	−5.26	0.00	−2.45
7	2.07	−5.26	0.00	−2.48
8	2.33	−5.26	0.00	−2.45
9	2.58	−5.26	0.00	−2.46
10	2.84	−5.26	0.00	−2.45
11	3.10	−5.26	0.00	−2.44
12	3.36	−5.26	0.00	−2.43
13	3.62	−5.26	0.00	−2.49
14	3.88	−5.26	0.00	−2.48
15	4.13	−5.26	0.00	−2.48
16	4.39	−5.26	0.00	−2.49
17	4.65	−5.26	0.00	−2.49
18	4.91	−5.26	0.00	−2.50
19	5.17	−5.26	0.00	−2.51
20	5.43	−5.26	0.00	−2.49
21	5.68	−5.26	0.00	−2.46
22	5.94	−5.26	0.00	−2.44
23	6.20	−5.26	0.00	−2.48
24	6.46	−5.26	0.00	−2.47
25	6.72	−5.26	0.00	−2.46
26	6.98	−5.26	0.00	−2.46
27	7.23	−5.26	0.00	−2.42
28	7.49	−5.26	0.00	−2.45
29	7.75	−5.26	0.00	−2.50
30	8.01	−5.26	0.00	−2.47
31	8.27	−5.26	0.00	−2.51
32	8.53	−5.26	0.00	−2.51
33	8.78	−5.26	0.00	−2.50
34	9.04	−5.26	0.00	−2.50
35	9.30	−5.26	0.00	−2.49
36	9.56	−5.26	0.00	−2.47
37	9.82	−5.26	0.00	−2.48
38	10.08	−5.27	0.00	−2.44

(mils per year) via Eq. (1) [14].

$$\text{Corrosion rate} = (W \times K)/(D \times A \times T) \quad (1)$$

Where W = mass loss (milligrams), $K = 534, D$ = density (g/cm^3), A = area (square inches), T = exposure time (hours).

A Gamry reference 600 Potentiostat/Galvanostat/ZRA was used for Potentiodynamic polarization experiments. The test set-up was designed in such a way as to diminish the consequence of high solution resistance by ensuring constant space amidst the working electrode and the reference electrodes. Duplicate tests were carried out in order to ascertain reproducibility of data. The Open circuit potential (OCP) and anodic polarization data are presented in Table 2 and Fig. 1 respectively. Figs. 3 and 4 shows the morphological images obtained after the tests.

3. Data, value and validation

The data reported in this paper is from weight loss (Fig. 1), open circuit potential (OCP) (Tables 1-3) and anodic polarization (Fig. 2) tests of MAS in E20 SFGE. The effect of chloride was assessed by conducting tests with and without chloride. For the data in this article, anodic polarization of MAS samples was effected by potentiodynamic polarization between −0.75 V vs SCE to 2.0 V vs SCE. Scanning was done at 2 mV/s. Data in this article is also for samples that after corrosion tests, the surfaces were characterized by morphological examination (Figs. 3-4). Fig. 1 shows the variation of corrosion rate of MAS with chloride ion concentration. In the absence of chloride, corrosion rate was 8.17×10^{-3} mils per year (mpy), but upon addition of 32 mg/L NaCl, corrosion rate increased from 8.17×10^{-3} mpy to 1.25×10^{-2} mpy. A further increase in chloride concentration to 64 mg/L increased corrosion rate of MAS to 1.96×10^{-2} mpy. Chloride ion in fuel ethanol is assumed to originate from the salt used in meal preparation in the course of bioethanol production [4]. Tables 1-3 show the OCP results obtained for micro-alloyed steel in the presence and absence of chloride. The role of the OCP in corrosion measurement is to indicate how stable the material was in the environment of interest. A comparison of the final voltage (Vf) obtained

Table 3
OCP Data for micro-alloyed steel in E20 + 64 mg/L NaCl.

Pt #	T s	Vf V vs. Ref. (E-01)	Vm V (*E* + 00)	Ach V (E-04)
0	0.26	−8.03	0.00	4.69
1	0.52	−8.03	0.00	4.66
2	0.78	−8.03	0.00	4.64
3	1.03	−8.03	0.00	4.66
4	1.29	−8.03	0.00	4.64
5	1.55	−8.04	0.00	4.66
6	1.81	−8.04	0.00	4.62
7	2.07	−8.04	0.00	4.65
8	2.33	−8.04	0.00	4.68
9	2.58	−8.04	0.00	4.68
10	2.84	−8.04	0.00	4.66
11	3.10	−8.03	0.00	4.64
12	3.36	−8.03	0.00	4.69
13	3.62	−8.03	0.00	4.65
14	3.88	−8.02	0.00	4.66
15	4.13	−8.02	0.00	4.67
16	4.39	−8.01	0.00	4.63
17	4.65	−8.00	0.00	4.63
18	4.91	−7.99	0.00	4.62
19	5.17	−7.98	0.00	4.64
20	5.43	−7.98	0.00	4.66
21	5.68	−7.99	0.00	4.68
22	5.94	−8.00	0.00	4.68
23	6.20	−8.00	0.00	4.64
24	6.46	−8.00	0.00	4.67
25	6.72	−8.00	0.00	4.64
26	6.98	−8.00	0.00	4.68
27	7.23	−8.00	0.00	4.64
28	7.49	−7.99	0.00	4.65
29	7.75	−7.98	0.00	4.60
30	8.01	−7.96	0.00	4.65
31	8.27	−7.96	0.00	4.66
32	8.53	−7.96	0.00	4.65
33	8.78	−7.97	0.00	4.63
34	9.04	−7.98	0.00	4.68
35	9.30	−7.99	0.00	4.66
36	9.56	−8.00	0.00	4.72
37	9.82	−8.00	0.00	4.67
38	10.08	−8.00	0.00	4.66

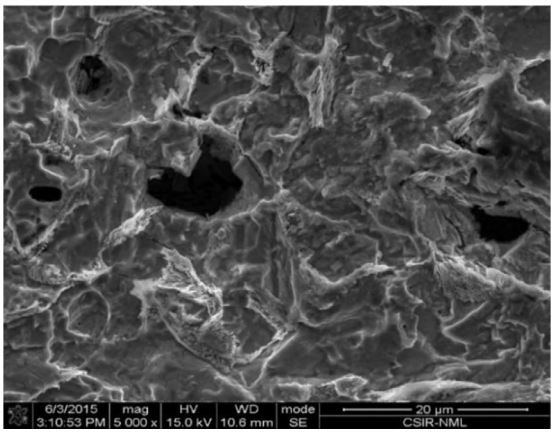

Fig. 4. Pitting of MAS through immersion test in the presence of chloride.

in Tables 1-3 shows decreasing Vf with increase in chloride concentration. The more positive potential (in the absence of chloride) signifies a more noble behaviour, which means the material is less affected by the fuel ethanol environment. This OCP result compares well with corrosion rate where we have the least corroded material in the absence of chloride.

Fig. 2 shows the polarization curves for MAS in the three chloride concentrations. MAS did not exhibit a distinct passivation behaviour and pitting potential with Potentiodynamic polarization in all the tests, which is expected due to the fact that metals usually show poor passive behaviour in alcoholic environments [18]. Fig. 3 shows the SEM image of MAS exposed to E20 + 0 mg/L NaCl where crazed cracks are seen due to shrinkage of the sample surface. Conversely, localized corrosion was obvious on MAS at 32 and 64 mg/L NaCl concentrations (Fig. 4). The localised corrosion was caused by the presence of the aggressive chloride ions in fuel ethanol [18].

Declaration of interests

The authors declare that they have no known competing financial interests or personal relationships that could have appeared to influence the work reported in this paper.

Acknowledgment

The authors acknowledge the funding received from CSIR-TWAS (FR No. 3240275047). Covenant University is recognized for open access funding.

References

[1] O.O. Joseph, Chloride effects on the electrochemical degradation of micro-alloyed steel in E20 simulated fuel ethanol blend, Results Phys. 7 (2017) 1446–1451.
[2] R.D. Kane, J.G. Maldonado, L.J. Klein, Stress corrosion cracking in fuel ethanol: a newly recognized phenomenon, Paper Presented at Corrosion 2004, NACE International, 2004.
[3] N. Sridhar, F. Gui, J.A. Beavers, J. James, Biofuels infrastructure, Managing in an Uncertain Future (DNV Research and Innovation - Position Paper 03), Det Norske Veritas, Hovik, Norway, 2010.
[4] L.M. Baena, M. Gomez, J.A. Calderon, Aggressiveness of a 20% bioethanol-80% gasoline mixture on autoparts: i behaviour of metallic materials and evaluation of their electrochemical properties, Fuel 95 (2012) 320–328.
[5] J.A. Beavers, M.P. Brongers, A.K. Agrawal, F.A. Tallarida, Prevention of internal SCC in ethanol pipelines, Paper presented at Corrosion 2008, NACE Conference & EXPO, 2008.
[6] J.G. Maldonado, R.D. Kane, Stress corrosion cracking of carbon steel in fuel ethanol service, Environ.-Induced Crack. Mater. 2 (2008) 337–347.
[7] Minnesota Pollution Control Agency. 2008. E20: the feasibility of 20 percent ethanol blends by volume as a motor fuel, executive summary results of materials compatibility and drivability testing. Minnesota, USA. Retrieved from http://www.ethanolrfa.org/wp-content/uploads/2015/09/
[8] X. Lou, D. Yang, P.M. Singh, Effect of ethanol chemistry on stress corrosion cracking of carbon steel in fuel-grade ethanol, Corrosion 65 (12) (2009) 785–797.
[9] L. Goodman, P.M. Singh, Effects of chemical composition of ethanol fuel on carbon steel pipelines, Paper Presented at the 11th International Conference on Advanced Materials (ICAM 2009), 2009.
[10] Venkatesh, A., Chambers, B., Kane, R.D., Kirkham, K. 2010. Evaluation of stress corrosion cracking behavior of steel in multiple ethanol environments. Paper P resented at Corrosion 2010, NACE International, San Antonio, Texas.
[11] L. Cao, Corrosion and Stress Corrosion Cracking of Carbon Steel in Simulated Fuel Grade Ethanol (Ph.D. thesis, Ohio State University, Ohio, USA, 2012.
[12] API Bulletin 939E. 2013. Identification, repair, and mitigation of cracking of steel equipment in fuel ethanol service (2nd ed.). Retrieved from www.techstreet.com
[13] National Research Council, Research Opportunities in Corrosion Science and Engineering, The National Academies Press, Washington D.C., 2011.
[14] ASTM G1-03, Standard practice for preparing, cleaning and evaluating corrosion test specimens, Annual Book of ASTM Standards, ASTM International, West Conshohocken, PA, USA, 2003.
[15] ASTM D-4806-07, Standard specification for denatured fuel ethanol for blending with gasolines for use as automotive spark ignition engine fuel, Annual Book of ASTM Standards, ASTM International, West Conshohocken, PA, USA, 2007.
[16] O.O. Joseph, C.A. Loto, S. Sivaprasad, J.A. Ajayi, S. Tarafder, Role of chloride in the corrosion and fracture behavior of micro-alloyed steel in E80 simulated fuel grade ethanol environment, Materials (Basel) 9 (2016) 463.
[17] O.O. Joseph, C.A. Loto, S. Sivaprasad, J.A. Ajayi, O.S.I. Fayomi, Comparative assessment of the degradation mechanism of micro-alloyed steel in E20 and E80 simulated fuel ethanol environments, in: AIP Conference Proceedings, 1758, 2016 p. 020019-1-9-6.
[18] X. Lou, P.M. Singh, Role of water, acetic acid and chloride on corrosion and pitting behaviour of carbon steel in fuel-grade ethanol, Corros. Sci. 52 (2010) 2303–2315.